

Molecular Pathogenesis of Genetic and Inherited Diseases

Disrupted Membrane Homeostasis and Accumulation of Ubiquitinated Proteins in a Mouse Model of Infantile Neuroaxonal Dystrophy Caused by PLA2G6 Mutations

Ibrahim Malik,* John Turk,[†] David J. Mancuso,[‡]
Laura Montier,* Mary Wohltmann,[†]
David F. Wozniak,^{§¶} Robert E. Schmidt,^{¶||}
Richard W. Gross,^{‡***††} and Paul T. Kotzbauer^{*¶||**}

From the Department of Neurology,* the Divisions of Endocrinology, Metabolism, and Lipid Research[†] and Bioorganic Chemistry and Molecular Pharmacology[‡] in the Department of Medicine, the Departments of Psychiatry[§] and Pathology and Immunology,[¶] Hope Center for Neurological Disorders,[¶] and the Department of Molecular Biology and Pharmacology,^{**} Washington University School of Medicine, St. Louis; and the Department of Chemistry,^{††} Washington University, St. Louis, Missouri

Mutations in the PLA2G6 gene, which encodes group VIA calcium-independent phospholipase A2 (iPLA₂β), were recently identified in patients with infantile neuroaxonal dystrophy (INAD) and neurodegeneration with brain iron accumulation. A pathological hallmark of these childhood neurodegenerative diseases is the presence of distinctive spheroids in distal axons that contain accumulated membranes. We used iPLA₂β-KO mice generated by homologous recombination to investigate neurodegenerative consequences of PLA2G6 mutations. iPLA₂β-KO mice developed age-dependent neurological impairment that was evident in rotarod, balance, and climbing tests by 13 months of age. The primary abnormality underlying this neurological impairment was the formation of spheroids containing tubulovesicular membranes remarkably similar to human INAD. Spheroids were strongly labeled with anti-ubiquitin antibodies. Accumulation of ubiquitinated protein in spheroids was evident in some brain regions as early as 4 months of age, and the onset of motor impairment correlated with a dramatic increase in ubiquitin-positive spheroids throughout the neuropil in nearly all brain regions. Furthermore accumulating ubiquitinated proteins were observed primarily in insoluble fractions

of brain tissue, implicating protein aggregation in this pathogenic process. These results indicate that loss of iPLA₂β causes age-dependent impairment of axonal membrane homeostasis and protein degradation pathways, leading to age-dependent neurological impairment. iPLA₂β-KO mice will be useful for further studies of pathogenesis and experimental interventions in INAD and neurodegeneration with brain iron accumulation. (Am J Pathol 2008, 172:406–416; DOI: 10.2353/ajpath.2008.070823)

Infantile neuroaxonal dystrophy (INAD), also known as Seitelberger's disease, is a human neurodegenerative disorder that typically begins within the first few years of life and leads to progressive impairment of movement and cognition. The pathological hallmark of the disease is the presence of large spheroids containing accumulated material primarily located in distal axons and nerve terminals. These pathological changes are widely distributed throughout the brain and are also often found in peripheral axons. A common feature of spheroids characterized by electron microscopy (EM) studies is the accumulation of membranes with tubulovesicular structure.^{1–7}

Many cases of INAD are also characterized by iron deposition in the globus pallidus and substantia nigra pars reticulata, indicating significant overlap with the spectrum of diseases classified as neurodegeneration with

Supported by the National Institutes of Health (National Institute of Neurological Disorders and Stroke (grant NS48924-01 to P.T.K. and Neuroscience Blueprint core grant NS057105 to Washington University), the McDonnell Center for Cellular and Molecular Neurobiology (grant to P.T.K.), the United States Public Health Service (grants R37-DK34388, P41-RR00954, P60-DK20579, and P30-DK56341 to J.T., and 5P01HL57278 to R.W.G.), and the Juvenile Diabetes Research Foundation (grant to R.E.S.).

Accepted for publication October 23, 2007.

Address reprint requests to Paul T. Kotzbauer, M.D., Ph.D., Department of Neurology, Washington University School of Medicine, Box 8111, 660 South Euclid Ave., St. Louis, MO 63110. E-mail: kotzbauerp@neuro.wustl.edu.

brain iron accumulation (NBIA). NBIA currently includes the genetic disorder pantothenate kinase-associated neurodegeneration and possibly other genetic and sporadic etiologies that have not yet been identified.

Morgan and colleagues⁸ recently reported genetic mapping in four families with INAD and NBIA and the subsequent identification of a total of 44 unique *PLA2G6* mutations in patients with either INAD or NBIA. Mutations were present in both alleles in all but one patient. In a few cases, both alleles were affected by early frame shift and stop codon mutations and predicted to cause complete loss of iPLA₂ β function, but there were also 32 missense mutations causing single amino acid substitutions.⁸ *PLA2G6* mutations have also been independently identified in two additional INAD families.⁹

PLA2G6 encodes the calcium-independent phospholipase A₂ β (iPLA₂ β) enzyme, also designated iPLA₂-VIA, which hydrolyzes the sn-2 ester bond in phospholipids to release a free fatty acid and a 2-lysophospholipid.¹⁰ Mice deficient in iPLA₂ β were originally generated and described by Bao and colleagues.¹¹ iPLA₂ β knockout (iPLA₂ β -KO) mice are born with an expected Mendelian distribution and appear to grow and develop normally. Male iPLA₂ β -KO mice have greatly reduced fertility because of impaired function of spermatozoa.¹¹ Pancreatic islet β -cell function in iPLA₂ β -KO mice is impaired under conditions of metabolic stress, such as administration of multiple low doses of the β -cell toxin streptozotocin or prolonged feeding of a high-fat diet, although blood insulin and glucose levels are appropriately regulated under normal circumstances.¹²

The recent reports of iPLA₂ β mutations underlying INAD and NBIA led us to investigate the possibility that iPLA₂ β -null mice might recapitulate the neurodegenerative features of human INAD. We report here that iPLA₂ β -KO mice develop progressive age-dependent impairment of sensorimotor function that is accompanied by progressive accumulation of tubulovesicular membranes and ubiquitinated protein in spheroids throughout the brain. These findings demonstrate that iPLA₂ β -KO mice are a valuable model for the neurodegenerative process underlying human INAD and provide further insight into disease pathogenesis.

Materials and Methods

Materials

Chemicals were obtained from Sigma (St. Louis, MO) unless otherwise indicated.

Animals

iPLA₂ β -KO mice were previously generated by insertion of the neomycin resistance gene into exon 9 of the mouse *iPLA₂ β* gene by homologous recombination.^{11,12} iPLA₂ β -KO and wild-type (WT) animals were obtained by mating heterozygote animals and genotyping by either Southern blot or polymerase chain reaction assay for the KO allele. Mice were housed and cared for in animal facilities administered through the Washington University Division of

Comparative Medicine. All animal procedures were performed according to protocols approved by the Washington University Animal Studies Committee.

Behavioral Tests

Neurological impairment of iPLA₂ β -KO mice was assessed in groups of mice at two different ages using tests (a battery of sensorimotor measures, 1-hour locomotor activity, rotarod) that we have previously described and shown to be sensitive for detecting ataxia and other sensorimotor deficits in mutant mice that are associated with altered functions in the cerebellum, striatum, neocortex, and other brain regions.^{13,14} The younger group consisted of nine mice of each genotype at 3.5 to 4 months old during testing, and the older group consisted of five mice of each genotype at age 12.5 to 13 months during testing. WT and KO animals were littermates in the 13-month-old group but not in the 4-month-old group.

Tissue Processing

Animals from different age groups ranging from 4 to 13 months were deeply anesthetized by intraperitoneal injection of ketamine/xylazine cocktail and tissues were fixed by intracardiac perfusion with phosphate-buffered saline (PBS) followed by 4% paraformaldehyde. Brain, spinal cord, skin, and muscle were harvested. Tissues were postfixed overnight in 4% paraformaldehyde. Fixed brains were cut into 2- to 3-mm coronal sections before routine paraffin embedding.

Immunohistochemistry

Six μ m sections were stained as previously described¹⁵ with the following primary antibodies: mouse monoclonal antibody (mAb) anti-ubiquitin 1510 (1:10,000; Chemicon, Temecula, CA), rabbit polyclonal anti-ubiquitin (1:2000; DAKO, Carpinteria, CA), and anti- α -synuclein 303 antibody¹⁶ (1:1000, a gift from Dr. Virginia M.-Y. Lee, University of Pennsylvania, Philadelphia, PA). Species-specific biotinylated secondary antibodies were applied followed by avidin-horseradish peroxidase, and the chromogenic substrate diaminobenzidine tetrahydrochloride (Vector Laboratories, Burlingame, CA) was used for detection of horseradish peroxidase. Sections were counterstained with hematoxylin.

Prussian Blue Staining

Brains sections were deparaffinized and incubated in a solution containing equal parts of 2% potassium ferrocyanide and 2% hydrochloric acid for 1 hour at room temperature. The sections were washed and counterstained with nuclear-fast red for 5 minutes.

Quantitation of Ubiquitin-Positive Spheroids

Coronal brain sections of iPLA₂ β -KO and WT mice, from three different age groups (4, 8, and 13 months) were

immunostained with rabbit polyclonal anti-ubiquitin antibody as above, omitting the final hematoxylin counterstain. Images of the striatum from eight randomly selected fields from each brain region (four fields on each side) were obtained at $\times 40$ magnification. Metamorph image analysis software (Molecular Devices, Sunnyvale, CA) was used to analyze each image separately. The images were subtracted for background staining, and all particles (spheroids) staining above background were counted. Average numbers were obtained for KO mice and multiplied by 25 to obtain the mean number of spheroids in the striatum per mm^2 . Spheroid densities for KO mice were reduced by averages obtained for WT mice to control for background values obtained with the image analysis method. Results were graphically displayed with Prism software (Graphpad, San Diego, CA).

Transmission EM

WT and KO mice, 8 months of age, were anesthetized with ketamine/xylazine and brains were removed after intracardiac perfusion with PBS followed by a chilled solution of 3% glutaraldehyde in cacodylate buffer. The tissues were fixed overnight in the same fixative at room temperature. Tissue from each region of interest was dissected into several 1-mm pieces and postfixed in buffered OsO_4 , dehydrated in graded alcohol solutions and propylene oxide, and embedded in Epon. One- μm -thick sections were examined by light microscopy after staining with toluidine blue. Thin sections were cut onto formvar-coated slot grids and stained with uranyl acetate and lead citrate and examined with a JEOL (Tokyo, Japan) 1200 electron microscope.

Biochemical Fractionation of Brain Tissue

Mice, 13 months of age, were deeply anesthetized and brains were removed and dissected to obtain samples of frontal cortex plus striatum or striatum alone. Tissue was frozen and then subsequently fractionated using a sequential biochemical extraction method as previously described.¹⁷ Two extractions were performed for each of five extraction solutions by homogenizing with 25 strokes in a Dounce homogenizer. Composition of solutions used for extraction were as previously described¹⁷ and were used in the following volume/tissue weight ratios: high salt (HS) (3 ml/g), HS with 1% Triton X-100 (3 ml/g), RIPA (3 ml/g), 2% sodium dodecyl sulfate (SDS) (1 ml/g), and 70% formic acid (1 ml/g). All buffers except formic acid contained freshly added protease inhibitor cocktail. Equal volumes of each fraction were analyzed by SDS-polyacrylamide gel electrophoresis and Western blotting using rabbit anti-ubiquitin antibody (1:1000, DAKO).

Results

Mice that do not express $i\text{PLA}_2\beta$ were previously generated and described by Bao and colleagues.¹¹ The mutant allele, generated by homologous recombina-

tion in embryonic stem cells, contains an inserted neomycin resistance gene in exon 9 of the mouse $i\text{PLA}_2\beta$ gene. In mice homozygous for the mutant allele, $i\text{PLA}_2\beta$ mRNA is undetectable in a variety of tissues examined, and $i\text{PLA}_2\beta$ protein is absent in all tissues examined, including brain.¹²

We observed $i\text{PLA}_2\beta$ -KO mice at a variety of ages for evidence of gait difficulty or motor impairment. Although younger KO mice displayed no clear evidence of impairment, abnormalities in gait and movement were consistently observed in KO mice older than 12 months. The gait of older KO mice appeared uncoordinated with increased body sway from side to side. KO mice also appeared to have mild difficulty when rearing and climbing.

Age-Dependent Development of Neurological Impairment in $i\text{PLA}_2\beta$ -KO Mice

We used a number of quantitative behavioral tests to characterize the age-dependent development of neurological impairment in $i\text{PLA}_2\beta$ -KO mice. $i\text{PLA}_2\beta$ -KO mice and WT control mice were evaluated at age 4 and 13 months in the rotarod test using stationary, constantly rotating, and accelerating rotational speed paradigms. In each test paradigm the length of time that mice were able to stay on the rotarod was determined in three successive trials performed 3 days apart.

In studies of 4-month-old mice, WT and KO mice performed similarly, but in 13-month-old mice there was profound impairment of KO mice relative to WT littermate controls in all three paradigms (Figure 1, A–F). Although 13-month-old $i\text{PLA}_2\beta$ -KO mice exhibited large deficits on the stationary and constant speed conditions, they still showed improved performance across time, indicating some motor learning capabilities during these easier tasks. The KO mice performed most poorly in the accelerating rotarod and did not improve with subsequent trials (Figure 1F).

Further characterization of 13-month-old $i\text{PLA}_2\beta$ -KO mice in sensorimotor tests revealed additional functional deficits. KO mice had significantly more difficulty than WT mice in maintaining balance on either a 0.75-cm-wide ledge or a 3-cm-diameter platform (Figure 2, A and B). KO mice had difficulty climbing to the top of a vertical screen and were able to remain upside down on an inverted screen for a significantly shorter period of time than WT mice (Figure 2, C and D). Climbing and agility also appeared impaired when KO mice were placed at the top of a vertical pole and assessed for the speed at which they were able to climb down the pole, although differences did not achieve statistical significance because of variability in performance of KO mice (Figure 2E).

KO mice displayed an increased level of spontaneous activity when ambulation was measured for 1 hour (Figure 2F). Further analyses indicated that the greatest differences between groups occurred during the first and second 10-minute time blocks (not shown), suggesting a greater reaction to novelty on the part of the $i\text{PLA}_2\beta$ -KO mice. This finding of altered activity levels on the part of

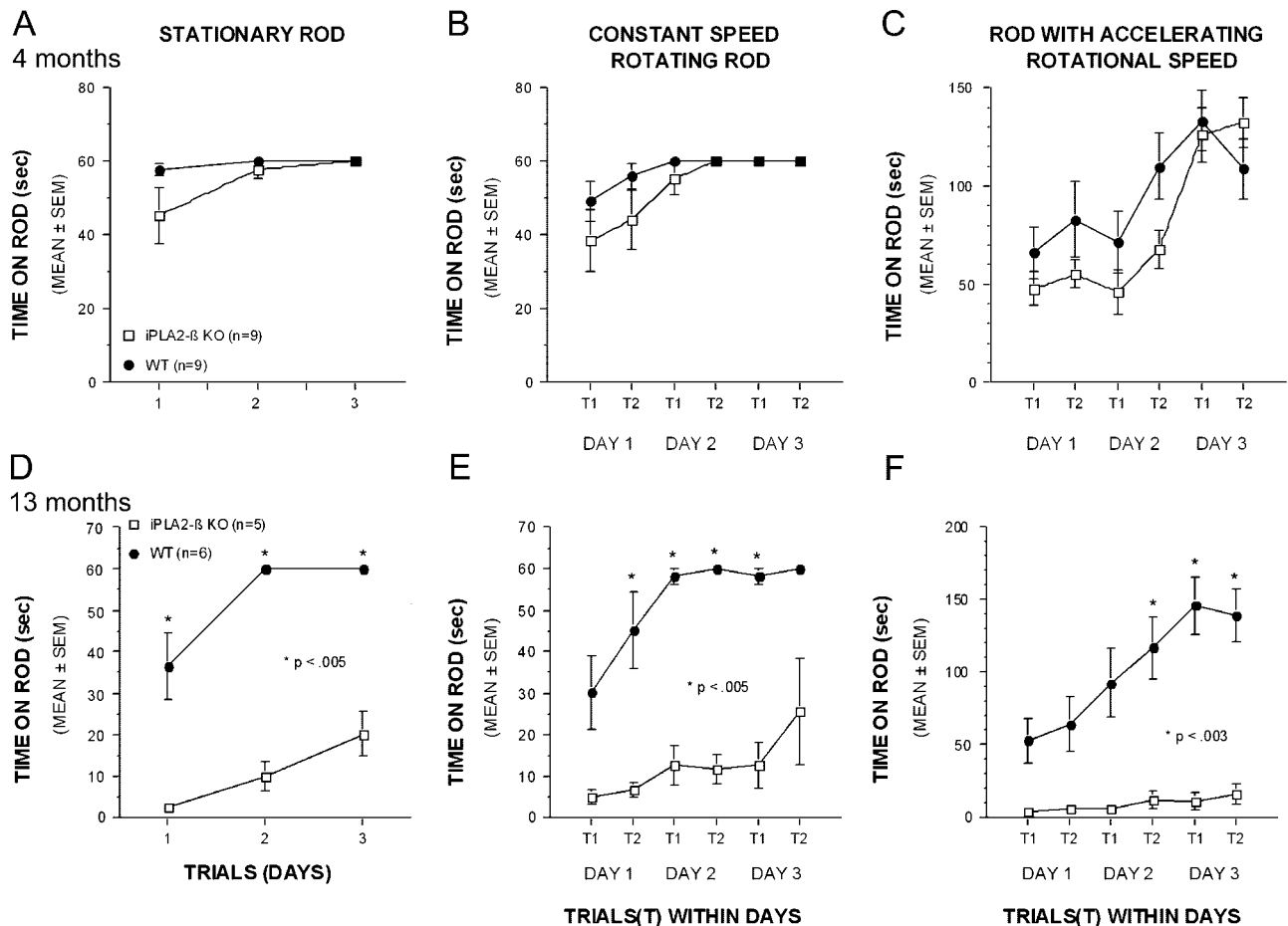


Figure 1. Age-dependent progression of neurological impairment in *iPLA₂β*-KO mice. Motor coordination and balance were assessed in groups of *iPLA₂β*-KO and WT mice, 4 and 13 months of age, with the rotarod test. **A–C:** The performance of 4-month-old KO mice was similar to WT mice on the stationary rod (**A**), the constant speed rotarod (**B**), and the accelerating rotarod (**C**) conditions. Although KO mice performed slightly worse during initial trials, no significant differences between the genotypes were observed at age 4 months. In addition, KO mice demonstrated improved performance across trials and test days suggesting motor learning capabilities, and their performance was equivalent to that of WT controls by the end of testing. **D–F:** In contrast to the 4-month-old KO mice, the performance of 13-month-old KO animals was profoundly impaired in all three rotarod conditions. Although the KO mice exhibited large and significant performance deficits on the stationary rod (**D**) and constant speed rotarod (**E**) conditions, they still showed improvement across trials and test days suggesting some motor learning capabilities. The performance of the KO mice was worst on the more challenging accelerating rotarod condition (**F**) where they showed no significant improvement during training. Asterisks in **D–F** indicate *P* values for pairwise comparisons between WT and KO genotypes.

the 13-month-old *iPLA₂β*-KO mice also suggests that the other functional deficits described above were not attributable to general malaise on the part of the *iPLA₂β*-KO mice.

Accumulation of Ubiquitinated Protein throughout the Brain in *iPLA₂β*-KO Mice

To investigate mechanisms of neurodegeneration underlying the age-dependent decline in motor function of *iPLA₂β*-KO mice, brain tissue from mice 4 to 13 months old was fixed and processed by paraffin embedding for histochemical and immunohistochemical analyses. Routine hematoxylin and eosin (H&E) staining of 6- μ m sections revealed no apparent anatomical differences between KO and WT mice. Cortical thickness and cerebellar granular and molecular layer thickness also appeared to be similar in both groups of mice.

Although infrequent eosinophilic spheroids were identified in some brain regions by H&E staining, immuno-

staining with anti-ubiquitin revealed a much greater number of spheroids throughout many brain regions. Examples of spheroids identified by anti-ubiquitin immunostaining of striatum in 8-month-old mice are shown in Figure 3. These round, ubiquitin-positive inclusions were present in many different brain regions, and were most abundant in striatum, cerebellum, and dorsal column nuclei at the youngest ages examined. As in human INAD, they were found primarily in the neuropil and often in a juxtaneuronal location, which suggests involvement of distal axons, although it is possible that dendritic processes are also affected.

Spheroids Contain Accumulating Membranes with Structure Similar to Human INAD

We used transmission EM to investigate the structure of spheroids found in the striatum of *iPLA₂β*-KO mice at 8 months of age. As shown in Figure 4, A–F, we found numerous spheroids with structural features remarkably

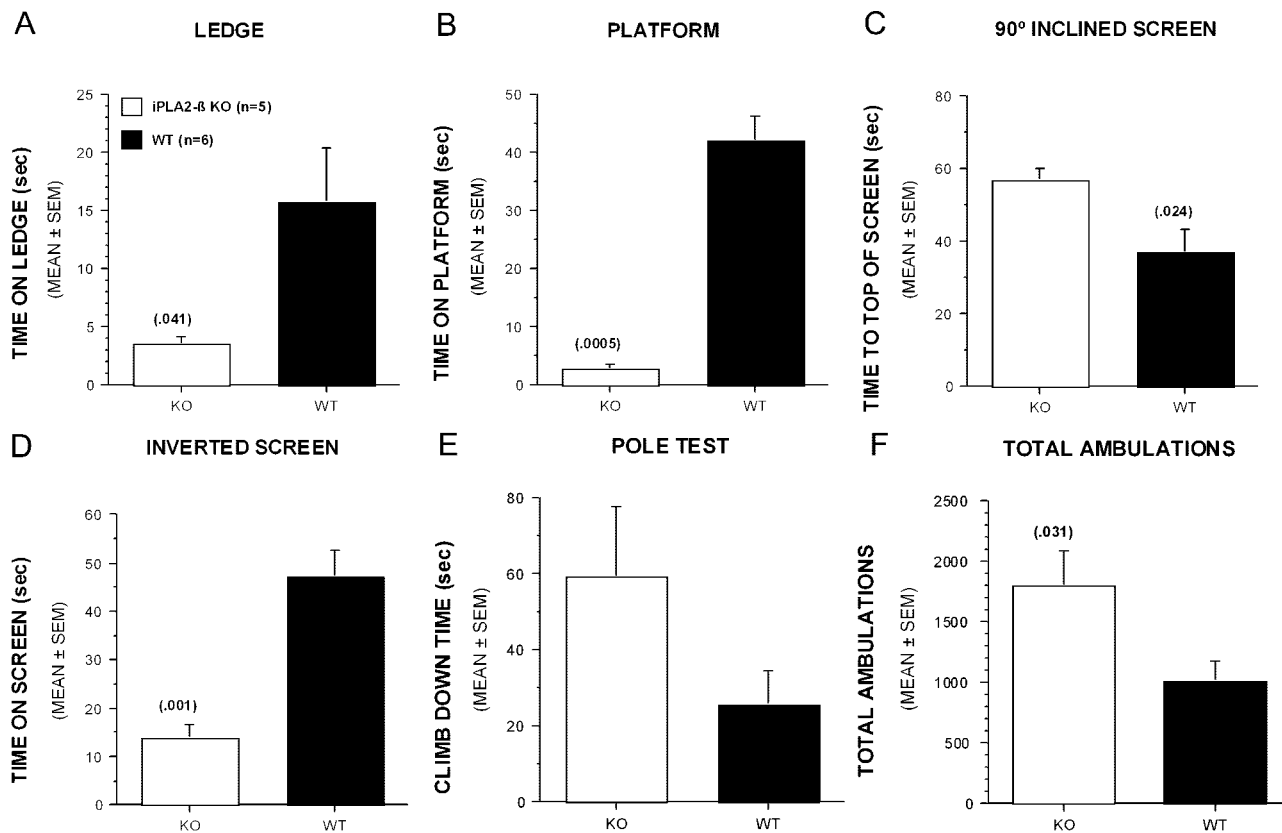


Figure 2. Thirteen-month-old *iPLA₂β*-KO mice are impaired in other sensorimotor tests involving balance, motor co-ordination, and strength, and they exhibited increased general locomotor activity. **A** and **B**: KO mice were able to remain on a narrow Plexiglas ledge (**A**) or a small circular platform (**B**) for significantly less time than WT littermate controls. **C** and **D**: KO mice also took significantly longer to turn and climb to the top of a 90° inclined screen (**C**) compared to WT littermates and were able to stay upside down on an inverted screen for a significantly shorter period of time compared to WT littermate controls (**D**). **E**: Although differences were not statistically significant, KO mice appeared to have greater difficulty in climbing down a vertical pole although their performance was highly variable. **F**: KO mice displayed significantly increased levels of general locomotor activity when total ambulations (whole body movements) were measured for 1 hour. Bars represent mean values and error bars represent SEM. *P* values are indicated in parentheses above error bars.

similar to those reported in human INAD. Spheroids in *iPLA₂β*-KO mice were typically found among small diameter axons and terminals in the neuropil and typically lacked a myelin sheath. The core structural appearance was one of accumulating densely compacted tubulovesicular elements, a term used to describe the appearance of an anastomosing network of delicate membrane structures with lumens. An additional consistent feature was the presence of a cleft that interrupted or bordered the tubulovesicular material. Clefts often contained sheets of membranes, sometimes found in stacked or whorled arrangements. These features are remarkably similar to those in human INAD.¹⁻⁷ Mitochondria were occasionally observed admixed within the tubulovesicular membranes. Some spheroids also contained separate regions of accumulated protein, mitochondria, and vesicles.

Ubiquitin staining and transmission EM also revealed pathological changes of neuroaxonal dystrophy in cerebellum, another brain region prominently affected in clinical and pathological studies of human INAD.^{18,19} Although there was no apparent atrophy or loss of neurons in the cerebellum, spheroids were present in the molecular layer and in juxtaneuronal locations in the Purkinje and granule cell layers. Transmission EM

revealed the same core feature of accumulating tubulovesicular membranes (Figure 4, G and H).

Age-Dependent Increase in Ubiquitin-Positive Spheroids throughout Multiple Brain Regions

Immunohistochemistry with anti-ubiquitin antibodies identified a consistent pattern of age-dependent increase in spheroids in three brain regions (Figure 5). At 4 months spheroids were small and relatively infrequent. With increasing age, ubiquitin-positive spheroids became more abundant and larger in these regions. Furthermore the distribution of spheroids became much more widespread with increasing age, and at 13 months, spheroids were numerous in nearly all cortical, subcortical, and brain-stem regions. We also observed spheroids in the spinal cord gray matter. With the exception of rare punctate ubiquitin-positive structures in cerebellum, ubiquitin-positive spheroids were not observed in WT animals at any of the ages examined.

The age-dependent accumulation of ubiquitinated protein in processes was assessed by image analysis of photomicrographs (Figure 6). These analyses indicated clear age-dependent increases in accumulation of ubi-

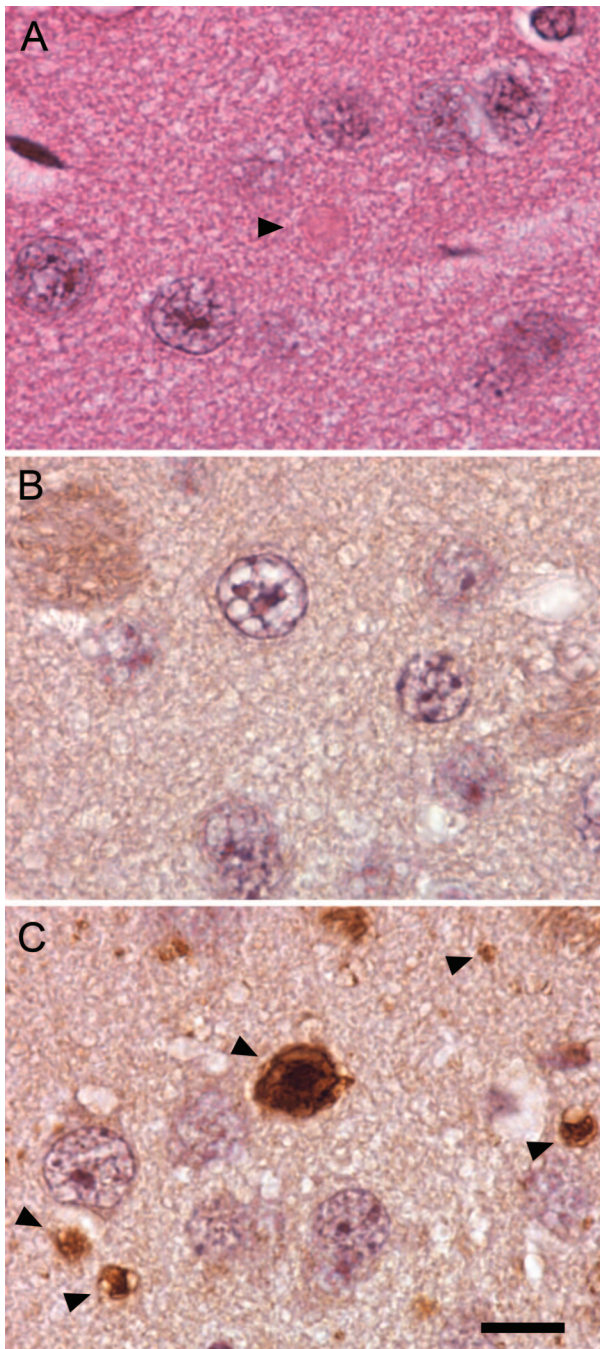


Figure 3. Spheroid formation in the striatum of iPLA₂β-KO mice. **A:** H&E staining of a striatum section from an iPLA₂β-KO mouse shows a round eosinophilic inclusion in the neuropil (arrowhead). **B** and **C:** Many more spheroids are visualized by immunohistochemistry using an antibody to ubiquitin compared to H&E staining. Comparison of ubiquitin staining in 8-month-old WT (**B**) and KO (**C**) mouse brain demonstrates numerous ubiquitin-positive spheroids in the neuropil of KO mice. Spheroids present in KO mouse brain, indicated by arrowheads, exhibit heterogeneous ubiquitin staining and range in size from 1 to 10 μm. Scale bar = 10 μm.

quintinated protein among different brain regions, with some variation in the rate of increase. Cerebellum was significantly affected by 4 months of age and there was a moderate increase between 4 and 13 months of age. Spheroid density in striatum increased consistently in the 4- to 8-month period and in the 8- to 13-month period. In

contrast, little involvement of cortex was present early, but between 8 and 13 months, ubiquitin-positive spheroids achieved densities in cortex that were comparable to or greater than those in other regions.

Ubiquitinated Proteins Accumulate in Insoluble Fractions of Brain Tissue

To characterize the biochemical properties of accumulating ubiquitinated proteins, we fractionated brain tissue by sequential extraction with buffers of increasing solubilization strength. Western blots of KO brain tissue fractions with anti-ubiquitin antibodies revealed the accumulation of ubiquitinated proteins that required the strong detergent SDS for extraction and solubilization (Figure 7). The pattern of accumulating high molecular weight protein species was complex, probably because of the presence of multiple polyubiquitinated proteins, and did not allow individual ubiquitinated protein species to be resolved. The localization of ubiquitinated proteins to SDS-soluble fractions suggests that protein misfolding and aggregation are involved in the process of spheroid formation.

Prominent Development of Spheroids in Regions also Affected by Neuroaxonal Dystrophy in Advanced Age and Diabetes

Because dystrophic changes are frequently observed in the peripheral nervous system in INAD, we examined the superior mesenteric and celiac ganglia of the sympathetic nervous system in iPLA₂β-KO mice by transmission EM. These peripheral sympathetic ganglia contained significant dystrophic changes with the same characteristic ultrastructural features observed in the central nervous system (Figure 8, A and B). Spheroids were also observed in axon terminals innervating the carotid body (not shown), but were not present in the superior cervical ganglion. The gracile and cuneate nuclei, which contain termini of dorsal root ganglia neurons, also contained prominent dystrophic changes that increased between 4 and 13 months of age (Figure 8, C and D). In humans and rodents, dystrophic changes in SMG, CG, and gracile nuclei have also been observed with advanced age.^{20,21}

Analysis of Pathological Iron and α-Synuclein Accumulation

A number of other pathological features often accompany spheroids in human INAD and NBIA, including iron accumulation in certain brain regions and the pathological accumulation of α-synuclein in Lewy bodies and Lewy neurites. In brain tissue from iPLA₂β-KO mice, Prussian blue staining for pathological iron accumulation did not provide evidence of iron accumulation in globus pallidus and substantia nigra. Pathological accumulation of α-synuclein in axonal and cytoplasmic inclusions, a finding that links both INAD and NBIA to Parkinson's disease and dementia with Lewy bodies,²²⁻²⁸ was ex-

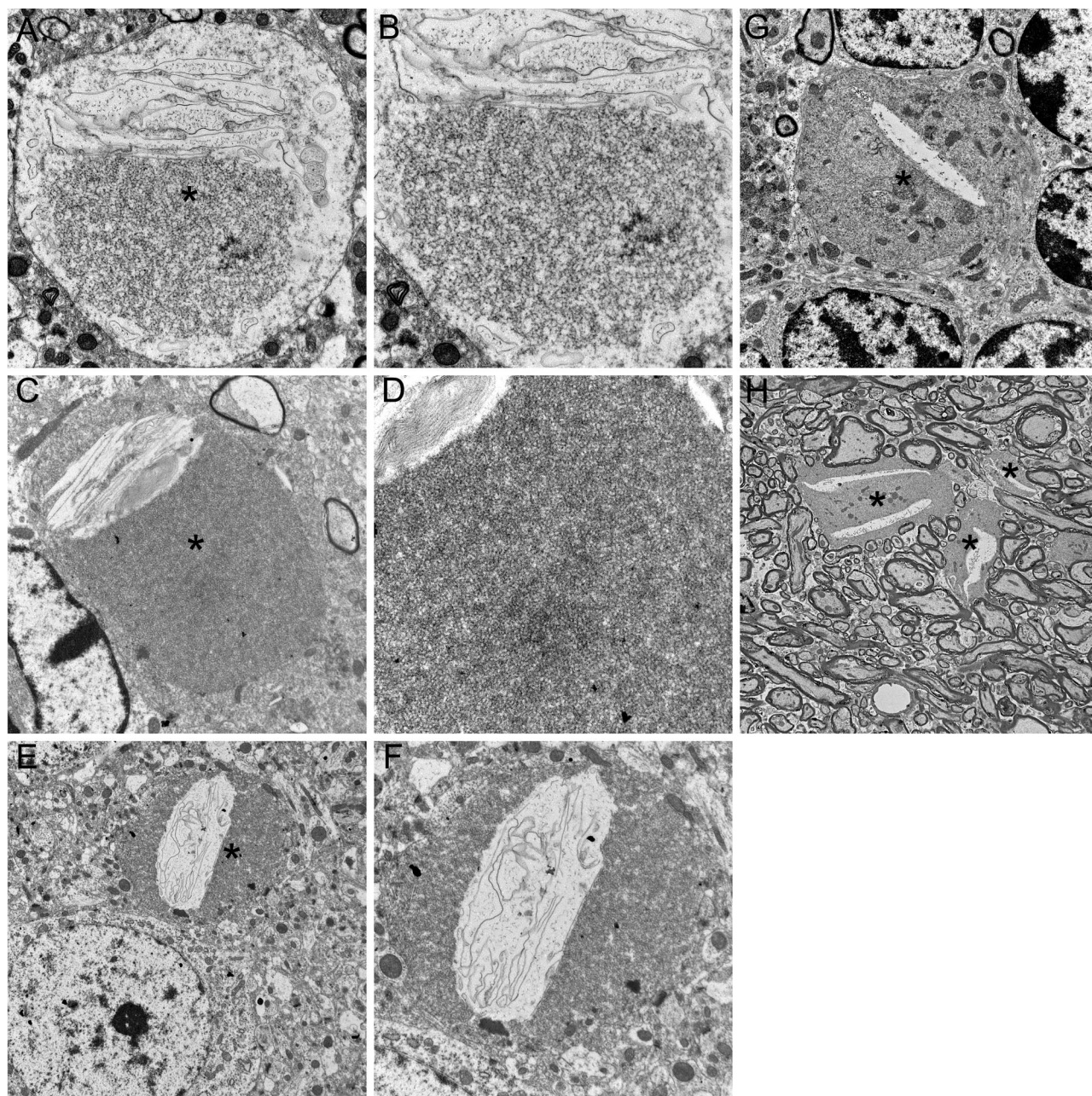


Figure 4. Transmission EM reveals tubulovesicular membranes and other material accumulating within spheroids. **A–F:** Images from transmission EM, performed on sections from striatum of 8-month-old KO and WT mice, illustrate ultrastructural features of spheroids. **B, D,** and **F** are higher magnification images of **A, C,** and **E,** respectively. Spheroids (asterisks) were typically surrounded by an intact membrane. Common to all spheroids was the presence of accumulating membranes. Tubulovesicular membranes were abundant and interrupted or bordered by clefts containing sheets of membranes, often in stacked or whorled structures. These structural features of spheroids strongly resemble those reported in human INAD. Transmission EM in the cerebellar granule layer (**G**) and molecular layer (**H**) also indicates accumulation of tubulovesicular membranes in spheroids. Magnifications: $\times 6400$ (**A, C, F**), $\times 8400$ (**B**), $\times 12,800$ (**D**), $\times 3200$ (**E**), $\times 4200$ (**G**), $\times 1280$ (**H**).

amined by immunohistochemistry. In WT and KO animals, similar diffuse staining of the neuropil was observed with α -synuclein antibodies. Although we have observed no evidence of Lewy bodies or dystrophic neurites using an antibody that preferentially recognizes pathological α -synuclein, syn303, we did observe accumulation of α -synuclein in spheroids, primarily in striatum, that appeared similar to those identified by ubiquitin staining (Figure 9). Staining of spheroids with syn303 was

less frequent than ubiquitin staining but was observed consistently.

Discussion

Discoveries of gene mutations underlying human neurodegenerative diseases provide unique opportunities to generate animal models through introduction of an

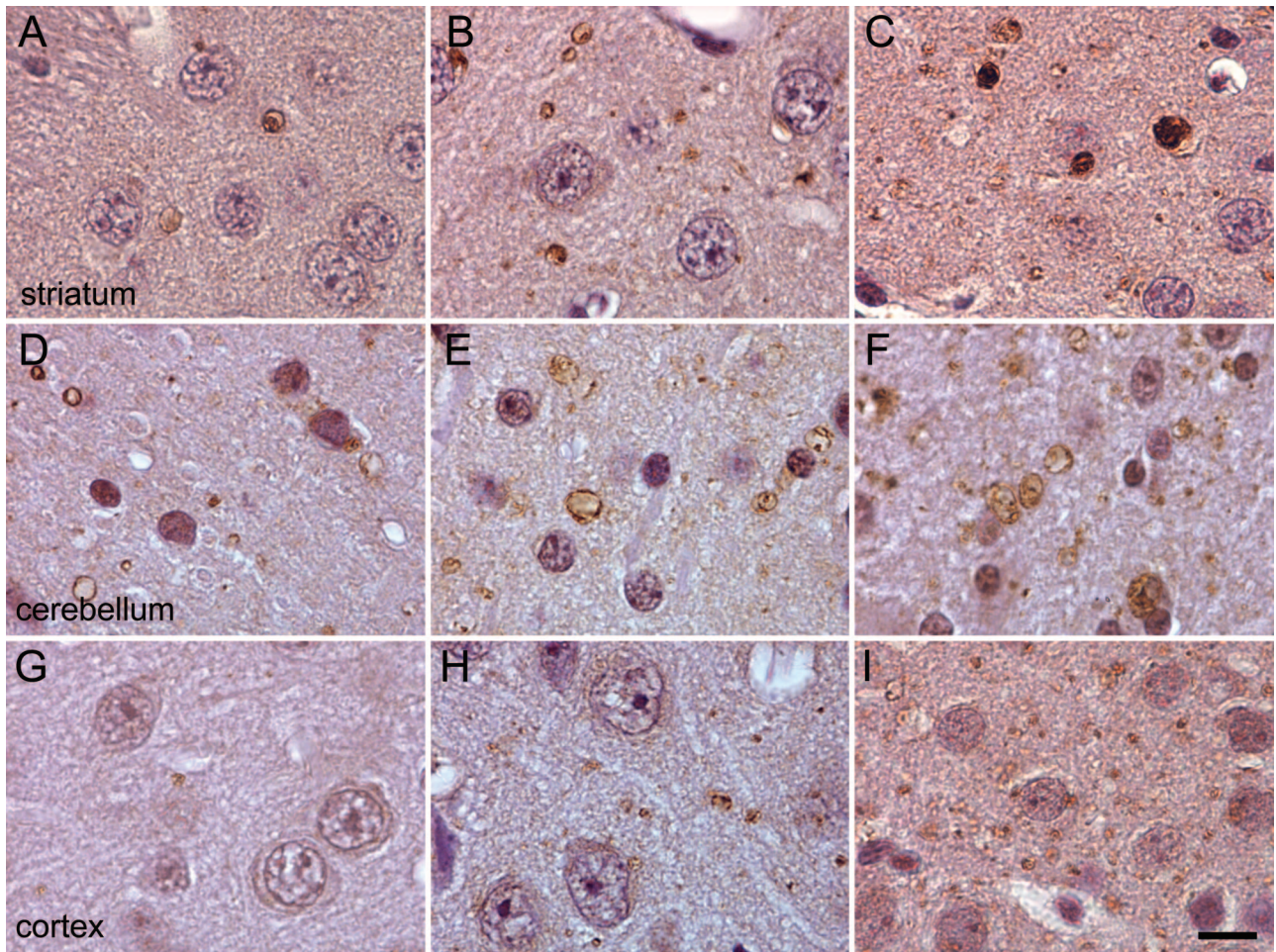


Figure 5. Age-dependent increase in spheroid density among multiple brain regions of *iPLA₂β-KO* mice as assessed by ubiquitin immunohistochemistry. Representative photographs from striatum (A–C), cerebellum (D–F), and cortex (G–I) are shown at ages 4, 8, and 13 months from left to right. A progressive increase in the density of ubiquitin-positive spheroids (labeled with brown diaminobenzidine tetrahydrochloride chromagen) in the neuropil was observed with increasing age in these regions and in nearly all other regions of the brain. Scale bar = 10 μ m.

orthologous gene defect in mice. Here we have investigated progressive neurodegeneration in *iPLA₂β-KO* mice and find that these mice model clinical and pathological features of human INAD caused by *PLA2G6* mutations. Progressive neurological impairment in *iPLA₂β-KO* mice correlates with progressive development of spheroids throughout the brain and peripheral nervous system. The accumulation of membranes with

tubulovesicular structure is remarkably similar to neuropathological findings previously reported in human INAD, and the accumulation of ubiquitinated proteins in spheroids has also been reported in one postmortem study of INAD.²⁹

The development of a mouse model for INAD provides significant opportunities for further studies of disease pathogenesis, as well as opportunities for preclinical test-

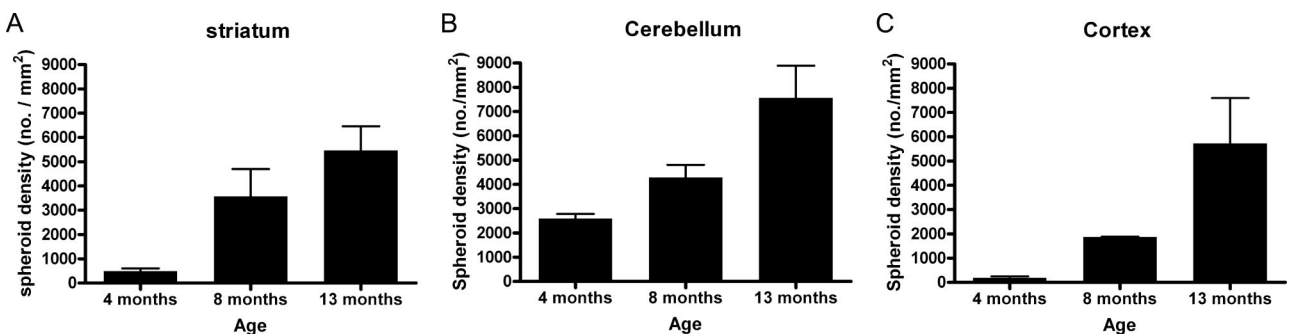


Figure 6. Quantitative assessment of progressive increases in spheroid density in striatum (A), cerebellum (B), and cortex (C) of *iPLA₂β-KO* mice. Brain sections from *iPLA₂β-KO* mice at 4, 8, and 13 months were stained with a rabbit polyclonal ubiquitin antibody, and average spheroid density in each region was determined by image analysis of multiple random fields in each region. Graphs show mean spheroid density at each age. Error bars indicate SD.

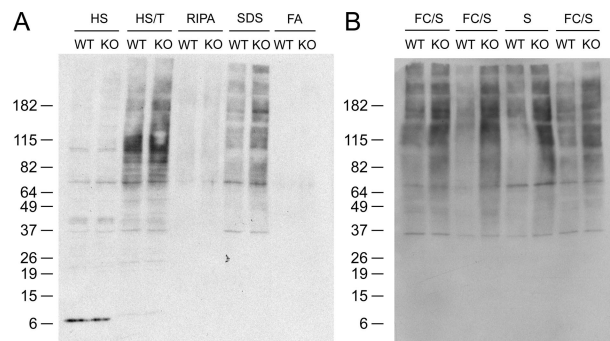


Figure 7. Ubiquitinated proteins accumulate in insoluble fractions obtained by sequential extraction of iPLA₂β-KO mouse brain. **A:** Anti-ubiquitin Western blot analysis of fractions obtained by sequential biochemical extraction of KO and WT mouse brain tissue samples containing frontal cortex plus striatum. The profiles of ubiquitinated proteins extracted by high salt (HS), high salt with Triton (HS/T), and RIPA buffers are similar, with perhaps a small increase in ubiquitinated proteins extracted from KO brain by HS/T. However there is a clear increase in a complex pattern of high molecular weight ubiquitinated protein species extracted by SDS buffer from KO brain tissue. The pattern of accumulating high molecular weight protein species was complex, indicating the presence of multiple polyubiquitinated proteins. **B:** Accumulation of ubiquitinated proteins in insoluble fractions was observed in multiple independent fractionation experiments using brain tissue samples containing frontal cortex plus striatum (FC/S) or striatum alone (S) from 13-month-old WT and KO mice.

ing of potential therapeutic interventions. The progressive neurodegenerative process in these mice can be assessed by quantitative behavioral tests of sensorimotor function and by quantitative assessment of ubiquitin-positive spheroids in the brain. Behavioral and pathological measures of disease progression could be used to investigate the effects of other genetic or metabolic factors linking the loss of iPLA₂β function to neurodegeneration.

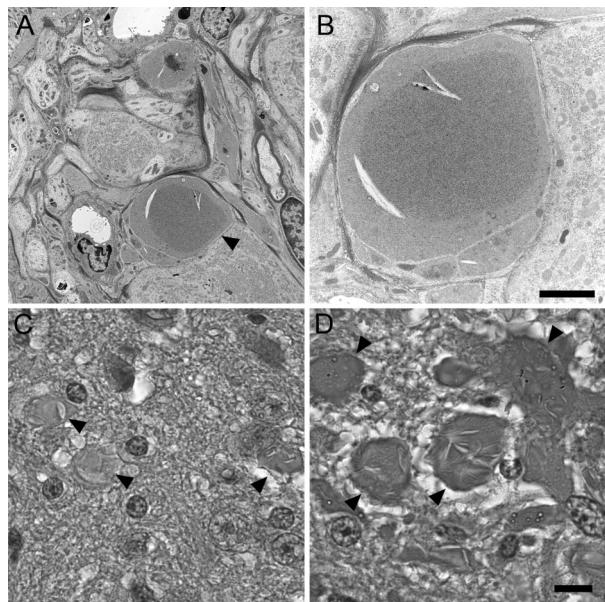


Figure 8. Neuroaxonal dystrophy affects the sympathetic nervous system and sensory axons in the gracile nucleus in iPLA₂β-KO mice. **A** and **B:** Images from transmission EM illustrate prominent spheroids with accumulating tubulovesicular membranes in axon terminals within the sympathetic superior mesenteric-celiac ganglia. H&E staining revealed large spheroids in the gracile nucleus at 4 months. **C:** Spheroids increased in size and number at 13 months (**D**). Scale bars: 6 μm (**A**); 2 μm (**B**); 10 μm (**C, D**).

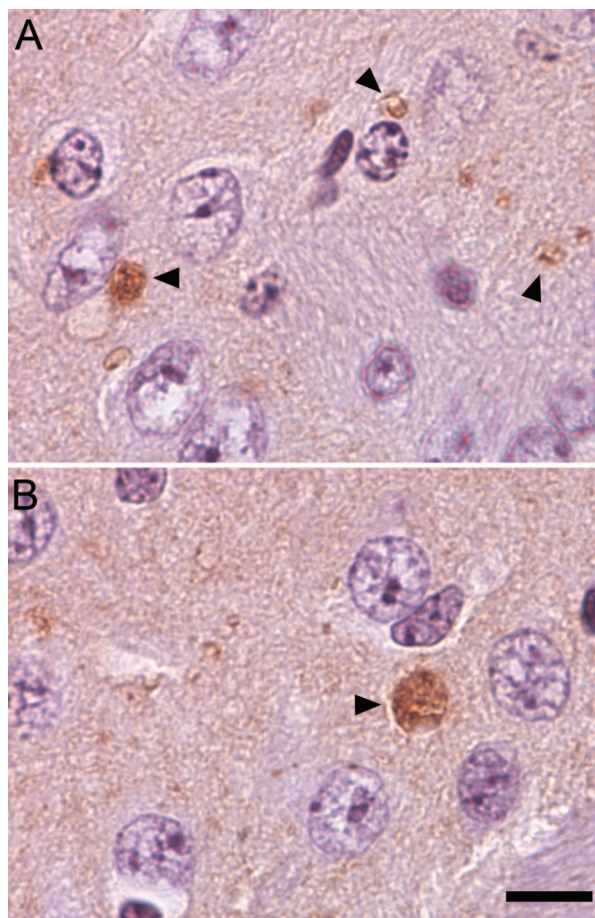


Figure 9. Accumulation of α-synuclein protein in spheroids in the striatum of iPLA₂β-KO mice. Immunohistochemistry using monoclonal synuclein antibody syn303 demonstrates staining of spheroids with morphology similar to those labeled with ubiquitin antibodies. Representative photographs (**A, B**) are shown from the striatum of a 13-month-old iPLA₂β-KO mouse. Syn303 staining was primarily observed in striatum of mice aged 13 months or older, with only rare staining of spheroids in other brain regions. Scale bar = 10 μm.

The widespread distribution of spheroids throughout the central and peripheral nervous system of iPLA₂β-KO mice resembles the widespread distribution observed in INAD. However, iPLA₂β-KO mice develop pathological and behavioral evidence of disease at a relatively later point within their lifespan than patients with human INAD, when disease onset is typically between 1 and 5 years of age. Spheroids are evident at 4 months of age in iPLA₂β-KO mice, and spheroid density progressively increases with age. Dysfunction in proprioceptive, cerebellar, and basal ganglia pathways reaches the threshold for significant impairment in sensorimotor function near the midpoint in the mouse lifespan. The shift in age dependence could be attributable to a number of factors that differ between mouse and human brain, such as axon length, number of synapses, and neuronal firing patterns, which may determine neuronal vulnerability to loss of iPLA₂β. Alternatively, age-dependent compensatory mechanisms may differ in mice and humans.

The primary pathogenic event caused by loss of iPLA₂β function is likely to be altered membrane composition. In addition to phospholipase A2 activity, iPLA₂β

also exhibits acyl CoA thioesterase activity.³⁰ Thus loss of this enzyme could lead to the accumulation of phospholipids and acyl CoAs, or to decreased release of free fatty acids, lysophospholipids, and free CoA. It is unclear whether specific molecular species within these classes of lipid molecules would be affected. Altered membrane composition attributable to changes in these classes of lipid molecules could have a number of downstream consequences through changes in membrane properties and could affect the function of membrane proteins including channels, transporters, receptors, and signaling enzymes.

Our results indicate that loss of membrane homeostasis leading to accumulation of membranes in distal axons underlies progressive neurological impairment in *iPLA₂β*-KO mice. Loss of *iPLA₂β* function could alter lipid composition of the plasma membrane, vesicles, or endosomes and thereby affect proteins and processes normally involved in regulating the movement of membranes within axons and dendrites. For example, endocytic or secretory pathways could be impaired by disruption of membrane budding, vesicle transport, or membrane fusion.

Ubiquitin immunohistochemistry is an early and sensitive marker of changes in *iPLA₂β*-KO mice. Furthermore, pathological ubiquitin immunostaining is accompanied by accumulation of ubiquitinated proteins in insoluble fractions prepared from KO brain tissue. Identification of individual protein species that accumulate in KO brain may provide further insight into changes in protein solubility and clearance because of loss of *iPLA₂β*. Altered protein solubility accompanies histopathological evidence of accumulating protein in many neurodegenerative diseases and reflects protein misfolding and aggregation.^{31,32} These intracellular inclusions are frequently labeled with anti-ubiquitin antibodies, suggesting a link between protein degradation pathways and accumulation of misfolded protein.

Accumulation of ubiquitinated proteins may be mechanistically linked to accumulation of membranes. Ubiquitination of membrane proteins initiates protein turnover through targeting to lysosomes.^{33–36} Altered membrane composition might result in membrane protein dysfunction and increased ubiquitination. Membrane composition changes could also cause misfolding and aggregation of membrane-associated proteins. Finally, it is possible that *iPLA₂β* is required for transport of ubiquitinated proteins for degradation by either lysosomes or the ubiquitin-proteasome system. For example, *iPLA₂β* deficiency might disrupt vesicle transport or sorting within endosomes and lead to accumulation of tubulovesicular membranes and associated ubiquitinated proteins.

The pathological features of neuroaxonal dystrophy are observed in a number of other settings that might provide further insight into mechanisms underlying this pathological process. Spheroids in the gracile nucleus and in the superior mesenteric and celiac ganglia are observed with advanced age in humans and rodents.^{20,21} Diabetes mellitus in humans and rodents also leads to neuroaxonal dystrophy in superior mesenteric and celiac ganglia.³⁷ A number of mouse models of neuroaxonal

dystrophy attributable to spontaneous mutations have also been reported,^{38–42} and they share the features of age-dependent development of motor and sensory impairment, accompanied by the pathological changes of neuroaxonal dystrophy in some neuronal populations, particularly those in the gracile nucleus.

In at least some neuronal populations, there thus may be multiple convergent pathways that ultimately lead to the final common destination of neuroaxonal dystrophy. It is possible that axon terminals in neuronal populations such as sympathetic ganglia and dorsal column nuclei are vulnerable to other environmental and genetic perturbations that converge on similar pathways involved in membrane homeostasis. A mutation in one of these mouse lines has been identified in the *Uchl1* gene, which encodes a ubiquitin carboxy-terminal hydrolase that may regulate levels of free monomeric ubiquitin,⁴² providing further support for the hypothesis that dysregulated protein ubiquitination or failed targeting of ubiquitinated proteins might play a central role in neuroaxonal injury and degeneration. Identification of the genetic defects in other mouse models^{38,39} might also provide further insight into pathways involved in these pathological processes.

A common feature linking many neurodegenerative disorders is the accumulation of misfolded and ubiquitinated proteins within neurons. The presence of other histopathological lesions in human INAD and NBIA, such as Lewy bodies and neurofibrillary tangles, further suggests that these diseases share mechanisms of pathogenesis with other disorders including Parkinson's disease and Alzheimer's disease. Although Lewy bodies and neurofibrillary tangles were not observed in *iPLA₂β*-KO mice, pathological accumulation of α -syn or tau might be further studied via transgenic expression of these proteins in *iPLA₂β*-KO mouse lines. Thus further studies of *iPLA₂β*-KO mice may provide significant insight into the role of altered lipid metabolism in a number of common sporadic neurodegenerative diseases in addition to INAD and NBIA.

Acknowledgments

We thank Karen Green for her excellent ultrastructural technical assistance and Sara Conyers for her excellent technical assistance with animal behavior studies.

References

1. Kimura S: Terminal axon pathology in infantile neuroaxonal dystrophy. *Pediatr Neurol* 1991, 7:116–120
2. Yagishita S, Kimura S: Infantile neuroaxonal dystrophy. Histological and electron microscopical study of two cases. *Acta Neuropathol (Berl)* 1974, 29:115–126
3. de Leon GA, Mitchell MH: Histological and ultrastructural features of dystrophic isocortical axons in infantile neuroaxonal dystrophy (Seitelberger's disease). *Acta Neuropathol (Berl)* 1985, 66:89–97
4. Yagishita S, Kimura S: Infantile neuroaxonal dystrophy (Seitelberger's disease). A light and ultrastructural study. *Acta Neuropathol (Berl)* 1975, 31:191–200
5. Liu HM, Larson M, Mizuno Y: An analysis of the ultrastructural findings

- in infantile neuroaxonal dystrophy (Seitelberger's disease). *Acta Neuropathol (Berl)* 1974, 27:201-213
6. Aicardi J, Castelein P: Infantile neuroaxonal dystrophy. *Brain* 1979, 102:727-748
 7. Ramaekers VT, Lake BD, Harding B, Boyd S, Harden A, Brett EM, Wilson J: Diagnostic difficulties in infantile neuroaxonal dystrophy. A clinicopathological study of eight cases. *Neuropediatrics* 1987, 18:170-175
 8. Morgan NV, Westaway SK, Morton JE, Gregory A, Gissen P, Sonek S, Cangul H, Coryell J, Canham N, Nardocci N, Zorzi G, Pasha S, Rodriguez D, Desguerre I, Mubaidin A, Bertini E, Trembath RC, Simonati A, Schanck C, Johnson CA, Levinson B, Woods CG, Wilmot B, Kramer P, Gitschier J, Maher ER, Hayflick SJ: PLA2G6, encoding a phospholipase A(2), is mutated in neurodegenerative disorders with high brain iron. *Nat Genet* 2006, 38:752-754
 9. Khateeb S, Flusser H, Ofir R, Shelef I, Narkis G, Vardi G, Shorer Z, Levy R, Galil A, Elbedour K, Birk OS: PLA2G6 mutation underlies infantile neuroaxonal dystrophy. *Am J Hum Genet* 2006, 79:942-948
 10. Akiba S, Mizunaga S, Kume K, Hayama M, Sato T: Involvement of group VI Ca²⁺-independent phospholipase A2 in protein kinase C-dependent arachidonic acid liberation in zymosan-stimulated macrophage-like P388D1 cells. *J Biol Chem* 1999, 274:19906-19912
 11. Bao S, Miller DJ, Ma Z, Wohltmann M, Eng G, Ramanadham S, Moley K, Turk J: Male mice that do not express group VIA phospholipase A2 produce spermatozoa with impaired motility and have greatly reduced fertility. *J Biol Chem* 2004, 279:38194-38200
 12. Bao S, Song H, Wohltmann M, Ramanadham S, Jin W, Bohrer A, Turk J: Insulin secretory responses and phospholipid composition of pancreatic islets from mice that do not express group VIA phospholipase A2 and effects of metabolic stress on glucose homeostasis. *J Biol Chem* 2006, 281:20958-20973
 13. Grady RM, Wozniak DF, Ohlemiller KK, Sanes JR: Cerebellar synaptic defects and abnormal motor behavior in mice lacking alpha- and beta-dystrobrevin. *J Neurosci* 2006, 26:2841-2851
 14. Wozniak DF, Hartman RE, Boyle MP, Vogt SK, Brooks AR, Tenkova T, Young C, Olney JW, Muglia LJ: Apoptotic neurodegeneration induced by ethanol in neonatal mice is associated with profound learning/memory deficits in juveniles followed by progressive functional recovery in adults. *Neurobiol Dis* 2004, 17:403-414
 15. Kotzbauer PT, Truax AC, Trojanowski JQ, Lee VM: Altered neuronal mitochondrial coenzyme A synthesis in neurodegeneration with brain iron accumulation caused by abnormal processing, stability, and catalytic activity of mutant pantothenate kinase 2. *J Neurosci* 2005, 25:689-698
 16. Giasson BI, Duda JE, Quinn SM, Zhang B, Trojanowski JQ, Lee VM: Neuronal alpha-synucleinopathy with severe movement disorder in mice expressing A53T human alpha-synuclein. *Neuron* 2002, 34:521-533
 17. Kotzbauer PT, Giasson BI, Kravitz AV, Golbe LI, Mark MH, Trojanowski JQ, Lee VM: Fibrillization of alpha-synuclein and tau in familial Parkinson's disease caused by the A53T alpha-synuclein mutation. *Exp Neurol* 2004, 187:279-288
 18. Jellinger K, Seitelberger F, Rosenkranz W: Infantile neuroaxonal dystrophy. Early form with preferential cerebellar involvement. *Acta Neuropathol (Berl)* 1968, 10:123-131
 19. Nardocci N, Zorzi G, Farina L, Binelli S, Scaioli W, Ciano C, Verga L, Angelini L, Savoiardo M, Bugiani O: Infantile neuroaxonal dystrophy: clinical spectrum and diagnostic criteria. *Neurology* 1999, 52:1472-1478
 20. Schmidt R: Neuroaxonal dystrophy in aging rodent and human sympathetic autonomic ganglia-synaptic pathology as a common theme in neuropathology. *Adv Pathol Lab Med* 1993, 6:505-522
 21. Schmidt RE, Chae HY, Parvin CA, Roth KA: Neuroaxonal dystrophy in aging human sympathetic ganglia. *Am J Pathol* 1990, 136:1327-1338
 22. Galvin JE, Giasson B, Hurtig HI, Lee VM, Trojanowski JQ: Neurodegeneration with brain iron accumulation, type 1 is characterized by alpha-, beta-, and gamma-synuclein neuropathology. *Am J Pathol* 2000, 157:361-368
 23. Neumann M, Adler S, Schluter O, Kremmer E, Benecke R, Kretschmar HA: Alpha-synuclein accumulation in a case of neurodegeneration with brain iron accumulation type 1 (NBIA-1, formerly Hallervorden-Spatz syndrome) with widespread cortical and brainstem-type Lewy bodies. *Acta Neuropathol (Berl)* 2000, 100:568-574
 24. Newell KL, Boyer P, Gomez-Tortosa E, Hobbs W, Hedley-Whyte ET, Vonsattel JP, Hyman BT: Alpha-synuclein immunoreactivity is present in axonal swellings in neuroaxonal dystrophy and acute traumatic brain injury. *J Neuropathol Exp Neurol* 1999, 58:1263-1268
 25. Saito Y, Kawai M, Inoue K, Sasaki R, Arai H, Nanba E, Kuzuhara S, Ihara Y, Kanazawa I, Murayama S: Widespread expression of alpha-synuclein and tau immunoreactivity in Hallervorden-Spatz syndrome with protracted clinical course. *J Neurol Sci* 2000, 177:48-59
 26. Wakabayashi K, Yoshimoto M, Fukushima T, Koide R, Horikawa Y, Morita T, Takahashi H: Widespread occurrence of alpha-synuclein/NACP-immunoreactive neuronal inclusions in juvenile and adult-onset Hallervorden-Spatz disease with Lewy bodies. *Neuropathol Appl Neurobiol* 1999, 25:363-368
 27. Wakabayashi K, Fukushima T, Koide R, Horikawa Y, Hasegawa M, Watanabe Y, Noda T, Eguchi I, Morita T, Yoshimoto M, Iwatsubo T, Takahashi H: Juvenile-onset generalized neuroaxonal dystrophy (Hallervorden-Spatz disease) with diffuse neurofibrillary and Lewy body pathology. *Acta Neuropathol (Berl)* 2000, 99:331-336
 28. Williamson K, Sima AA, Curry B, Ludwin SK: Neuroaxonal dystrophy in young adults: a clinicopathological study of two unrelated cases. *Ann Neurol* 1982, 11:335-343
 29. Bacci B, Cochran E, Nunzi MG, Izeke E, Mizutani T, Patton A, Hite S, Sayre LM, Utilio-Gambetti L, Gambetti P: Amyloid beta precursor protein and ubiquitin epitopes in human and experimental dystrophic axons. Ultrastructural localization. *Am J Pathol* 1994, 144:702-710
 30. Jenkins CM, Yan W, Mancuso DJ, Gross RW: Highly selective hydrolysis of fatty acyl-CoAs by calcium-independent phospholipase A2beta. Enzyme autoacylation and acyl-CoA-mediated reversal of calmodulin inhibition of phospholipase A2 activity. *J Biol Chem* 2006, 281:15615-15624
 31. Forman MS, Trojanowski JQ, Lee VM: Neurodegenerative diseases: a decade of discoveries paves the way for therapeutic breakthroughs. *Nat Med* 2004, 10:1055-1063
 32. Neumann M, Sampathu DM, Kwong LK, Truax AC, Micsenyi MC, Chou TT, Bruce J, Schuck T, Grossman M, Clark CM, McCluskey LF, Miller BL, Masliah E, Mackenzie IR, Feldman H, Feiden W, Kretschmar HA, Trojanowski JQ, Lee VM: Ubiquitinated TDP-43 in frontotemporal lobar degeneration and amyotrophic lateral sclerosis. *Science* 2006, 314:130-133
 33. Huang F, Kirkpatrick D, Jiang X, Gygi S, Sorkin A: Differential regulation of EGF receptor internalization and degradation by multiubiquitination within the kinase domain. *Mol Cell* 2006, 21:737-748
 34. Palacios F, Tushir JS, Fujita Y, Souza-Schorey C: Lysosomal targeting of E-cadherin: a unique mechanism for the down-regulation of cell-cell adhesion during epithelial to mesenchymal transitions. *Mol Cell Biol* 2005, 25:389-402
 35. Sharma M, Pampinella F, Nemes C, Benharouga M, So J, Du K, Bache KG, Papsin B, Zerangue N, Stenmark H, Lukacs GL: Misfolding diverts CFTR from recycling to degradation: quality control at early endosomes. *J Cell Biol* 2004, 164:923-933
 36. Walrafen P, Verdier F, Kadri Z, Chretien S, Lacombe C, Mayeux P: Both proteasomes and lysosomes degrade the activated erythropoietin receptor. *Blood* 2005, 105:600-608
 37. Schmidt RE: Neuropathology and pathogenesis of diabetic autonomic neuropathy. *Int Rev Neurobiol* 2002, 50:257-292
 38. Matsushima Y, Kikuchi T, Kikuchi H, Ichihara N, Ishikawa A, Ishijima Y, Tachibana M: A new mouse model for infantile neuroaxonal dystrophy, inad mouse, maps to mouse chromosome 1. *Mamm Genome* 2005, 16:73-78
 39. Bouley DM, McIntire JJ, Harris BT, Tolwani RJ, Otto GM, DeKruyff RH, Hayflick SJ: Spontaneous murine neuroaxonal dystrophy: a model of infantile neuroaxonal dystrophy. *J Comp Pathol* 2006, 134:161-170
 40. Bronson RT, Sweet HO, Spencer CA, Davisson MT: Genetic and age related models of neurodegeneration in mice: dystrophic axons. *J Neurogenet* 1992, 8:71-83
 41. Mukoyama M, Yamazaki K, Kikuchi T, Tomita T: Neuropathology of gracile axonal dystrophy (GAD) mouse. An animal model of central distal axonopathy in primary sensory neurons. *Acta Neuropathol (Berl)* 1989, 79:294-299
 42. Saigoh K, Wang YL, Suh JG, Yamanishi T, Sakai Y, Kiyosawa H, Harada T, Ichihara N, Wakana S, Kikuchi T, Wada K: Intragenic deletion in the gene encoding ubiquitin carboxy-terminal hydrolase in gad mice. *Nat Genet* 1999, 23:47-51